International Journal of Engineering Research and Technology. ISSN 0974-3154, Volume 12, Number 12 (2019), pp. 2574-2580

A Simple and Novel Automatic Marker Generation Algorithm for the Watershed Image Segmentation

Manikanta Prahlad Manda[a], Hi Seok Kim[b,*]

[a,b] Department *of Electronic Engineering, Cheongju University, Cheongju, 360-764, South Korea.*

ORCID: 0000-0002-3557-2944 (Manikanta), 0000-0002-5572-9320 (Hi Seok)

Abstract

A marker-based watershed algorithm is an efficient image segmentation method and has been widely used in many image processing applications. Most of the marker-based watershed methods require manual selecting the markers which need human interaction. To make the image segmentation completely automatic, we propose a new automatic markers generation method for the marker-based watershed algorithm. This algorithm uses gray-scale image histogram information and Otsu threshold information for generating the markers. The algorithm has been tested on images obtained from standard databases and experimental results show that the proposed method has the potential to outperform other existing image segmentation methods.

Keywords: Image segmentation; markers; gray-scale image histogram, Otsu threshold; watershed algorithm.

1. INTRODUCTION

Image segmentation is one of the most important tasks in machine vision application and at the same time image segmentation is the most difficult part of the image processing. Image segmentation is a process of subdividing an image into its constituent parts or objects. The objects contain some information and this information is useful in high-level machine vision applications.

In general, the image segmentation techniques are defined based on three principal concepts: (1) detecting discontinuities in gray levels, (2) image thresholding and (3) region-based segmentation. Some advantages and disadvantages are found for these methods when they had been used for image segmentation. Morphological watersheds combine some of the positive attributes of the three approaches for producing more stable segmentation results. The watershed algorithm generally leads to over-segmentation and this problem can be avoided by incorporating the concept of markers.

Markers can be generated either by manual selection or by using automatic generation algorithms. Automatic marker generation algorithms are needed in the implementation of real-time applications. Various approaches have been proposed for generating the markers automatically. In the traditional watershed algorithm, local minimum points in the gradient image are used as markers. Due to the imposition of the invalid markers leads to over-segmentation in the traditional watershed algorithm. In [17], Veta et al. proposed a marker-controlled watershed algorithm based on the radial symmetry transform. This method works well for the images containing symmetrical objects. The method is not suitable for the images containing unsymmetrical objects. Xiaoding et al. [20] proposed a marker-based watershed algorithm. In this method, the threshold value to find the markers is defined based on the percentage value. The percentage value varies between 0 and 1 and the selection of this value depends on the type of the image. Indirectly it needs human interaction for the segmentation of different type of images. Xiaoqiang et al. [10] proposed an improved watershed algorithm. In this method, the Otsu threshold is used for the rough segment the image and then the seed points for the watershed algorithm are calculated based on chamfer template distance transform. This method requires a large size chamfer template for producing accurate segmentation, but the complexity of this method increases as the size of the chamfer template increases. Muhammad et al. [22] proposed a watershed algorithm based on improved HSV transform. In this method, the Otsu thresholding approach is used to select values for the H, S and V components. This method was specially designed to extract the red colored objects in the image. This method suits only if the image has red-colored objects. This method is unable to perform well for extracting the multi-colored objects or extracting the objects other than red color. In [19], Girish et al. proposed a marker-controlled watershed algorithm based on k-means clustering. This method suffers from the over-segmentation problem for small values of *k*. A major difficulty of this method is selecting the value for *k*. We proposed a novel solution to overcome the aforementioned disadvantages and limitations. In the proposed method, simple mathematical analysis is used to extract valid markers. Only two parameters are needed to determine the marker set. One parameter has been used to determine the internal marker set and another parameter to determine the external marker set. The concept of statistical approach has been employed to determine the two parameters in the proposed method.

The proposed method is tested on various images exhibiting multimodal distribution in their histograms. Also, the proposed method is tested on mammographic images and infrared images. To evaluate the performance of the proposed method, the experiment results have been compared with the other image segmentation approaches (Otsu thresholding approach, edge-based image segmentation, traditional watershed algorithm). In our paper, two parameters (MSE and JI) have been taken for evaluating the performance of the proposed method. The proposed method produced satisfactory results. This paper is organized as follows. Section 2 gives a brief overview of basic principles and working of the various image segmentation methods. We propose a new procedure for the marker generation in section 3. The experimental results of the proposed method are analyzed in section 4. Our conclusions are drawn in the final section.

2. LITERATURE REVIEW

Image segmentation is an important task in image analysis. The image segmentation techniques are broadly classified into two categories: discontinuity based and similarity-based. The Watershed algorithm is developed by taking some positive attributes of the different image segmentation techniques.

2.1. Otsu method

Otsu method is one of the simplest ways to perform image segmentation and it is used extensively in many applications. Otsu method is a similarity-based image segmentation technique, it divides the pixels based on the predefined threshold value. Otsu threshold method identifies the optimal threshold value by making use of the histogram of the image. The intensity value which maximizes the measure of between-class variance is defined as the Otsu threshold [1, 9].

$$\sigma_B^2(t^*)_{T_{\text{Otsu}}=t^*} = Arg \max_{0 \le t \le L-1} \sigma_B^2(t) \tag{1}$$

Here $\sigma_B^2(t)$ is the between-class variance function and *t* is the intensity value ranging from 0 to L-1.

Otsu method allows misclassification errors in the case of multimodal histograms with no sharp or well-defined edges which is one of the main drawbacks of this method.

2.2. Edge-based image segmentation

Edge-based image segmentation technique is a discontinuity based image segmentation technique and it works based on the principle of detecting meaningful discontinuities in gray level of the image. A set of connected pixels located at the boundary between two regions represent an edge. Edge-based image segmentation method uses gradient operator and Laplacian operator in analyzing the image characteristics. Edge-based image segmentation techniques are unsuccessful if the image is noisy or its characteristics differ by a small amount between regions. The proposed method reduces the problems that arise in the edge-based image segmentation methods [6].

2.3. Morphological Watershed algorithm

The Watershed algorithm is first introduced by Beucher and Vincent based on mathematical morphology [2]. The Watershed algorithm incorporates many positive attributes of the other image segmentation techniques to give improved segmentation outputs. The boundaries formed in the Watershed algorithm are continuous with no gaps and they are formed naturally out of the process. The Watershed algorithm produces stable segmentation results.

In the watershed algorithm [14, 18], the image is considered as three-dimensional surfaces with two spatial dimensions and one dimension is intensity value at each pixel. The intensity values on the spatial surface form a topography on the spatial surface. Low-intensity values on the spatial surface will form a shallow relief and high-intensity values on the spatial surface will form mountains. The topography of the image will have minimum points and maximum points. The set of points on image topography is defined as regional minima and the set of points around this regional minimum point constructs the catchment basin or watershed of that minimum. Dams are built to separate to avoid amalgamation of the intensities from different catchment basins. The process of flooding of intensity values in the catchment basins starts at the local minimum points corresponding to each of the catchment basins and stops when the intensity levels have reached the highest gray-level. Local irregularities present in the image gradient generally lead to over-segmentation in the watershed algorithm. One way to control the over-segmentation by using the concept of markers in the Morphological watershed algorithm.

Finding the valid regional minima is the key to controlling the over-segmentation problem in the watershed algorithm. Markers are the valid regional minima and after selecting the markers, all the invalid regional minima are omitted and this way the over-segmentation problem is reduced in the watershed algorithm. A set of markers can be selected either by manual selection or using various automatic marker generation algorithms.

Although a manual selection of markers gives accurate segmentation results, they are time-consuming as they need human interaction for selecting the markers. Automatic marker generation algorithms avoid human intervention for selecting the markers. In recent years, there has been a considerable number of automatic marker generation algorithms for the watershed segmentation method, only a few algorithms are giving accurate segmentation. In this paper, we proposed an automatic markers generation technique. The next section explains the automatic marker generation in detail and the subsequent section discusses experimental results.

3. PROPOSED METHOD

In the proposed method only two parameters are required to determine the entire marker set. One parameter is the highest value in the internal marker set (k_{R_1}) and another parameter is the least value of the external marker set (k_{R_2}). We used gray-scale image histogram and Otsu threshold value in order to determine the values for k_{R_1} and k_{R_2} in the proposed method. The marker sets obtained from the values of k_{R_1} and k_{R_2} are imposed as initial seed-points in the catchment basins of the gradient image. Each catchment basin is marked out by either internal marker set or external marker set.

3.1. Marker generation

Markers are the initial sources for the marker-based watershed segmentation method. Markers in the watershed algorithm are classified into two categories: internal markers and external markers. The background (dark) of the image is labeled by the internal markers and the foreground (bright) of the image is labeled by the external markers (bright). Gray-scale histogram of the image is used for extracting the markers.

An image can be represented in a three-dimensional Cartesian coordinate system. The coordinates x and y represents the spatial dimensions of the pixels in the image and $f(x,y)$ represents the intensity of the pixel located at the point (x,y). The two-dimensional space created by the coordinates x and y is denoted as $\mathbf{Z}^2$. A graph between the gray-scale intensities and the number of pixels associated with each gray-scale intensity is defined as the histogram of the image.

In the proposed method, the image has been converted to gray-scale in order to find gray-scale histogram and the Otsu threshold value (T_{Otsu}). The image is divided into two clusters based on Otsu threshold value as cluster 1 and cluster 2. Cluster 1 contains all the pixels possessing intensity value less than or equal to the Otsu threshold value and cluster 2 contain all the pixels possessing intensity value greater than the Otsu threshold value. The spatial coordinates associated with the cluster 1 and cluster 2 are represented as,

$$R_1(f) = \{(x,y) \in \mathbf{Z}^2 \mid f(x,y) \le T_{\text{Otsu}}\} \tag{2}$$

$$R_2(f) = \{(x,y) \in \mathbf{Z}^2 \mid f(x,y) > T_{\text{Otsu}}\} \tag{3}$$

Here, $R_1(f)$ represents the set of pixel coordinates in cluster 1 and $R_2(f)$ represents the set of pixel coordinates in cluster 2.

The average of the number of pixels present in the region $R_1(f)$ is determined as

$$\overline{r_1} = \frac{1}{T_{\text{Otsu}}}\sum_{i=0}^{T_{\text{Otsu}}} i n_i \tag{4}$$

Here i is the pixel's intensity at a point (x,y) and n_i is the number of pixels corresponding to the intensity level i.

Consider the all gray-scale intensities which are having the number pixels less than the average value $\overline{r_1}$ in the region $R_1(f)$. The highest value of the internal-marker set is determined as follows.

$$k_{R_1} = \frac{\sum_{n_i<\overline{r_1}, i\in R_1(f)} i n_i}{\sum_{n_i<\overline{r_1}, i\in R_1(f)} n_i} \tag{5}$$

The set of internal marker coordinates of the watershed is determined from the value of k_{R_1} as follows.

$$M_1\left[k_{R_1}\right] = \left\{(x,y) \in \mathbf{Z}^2 \mid f(x,y) \le k_{R_1}\right\} \tag{6}$$

The average number of pixels present in the region $R_2(f)$ is determined as

$$\overline{r_2} = \frac{\sum_{i=T_{\text{Otsu}}+1}^{L-1} i n_i}{(L-1)-(T_{\text{Otsu}}+1)} \tag{7}$$

Here, L is the highest gray-scale intensity of the image.

Consider all gray-scale intensities in the region $R_2(f)$ which are having the number of pixels less than the average value of the pixels$(\overline{r_2})$. The least value of the external-marker set is determined as follows.

$$k_{R_2} = \frac{\sum_{n_i<\overline{r_2}, i\in R_2(f)} i n_i}{\sum_{n_i<\overline{r_2}, i\in R_2(f)} n_i} \tag{8}$$

And the set of external marker coordinates of the watershed is determined from the value of k_{R_2} as follows.

$$M_2\left[k_{R_2}\right] = \left\{(x,y) \in \mathbf{Z}^2 \mid f(x,y) \ge k_{R_2}\right\} \tag{9}$$

Finally, the marker set for controlling the watershed algorithm is the union of the internal marker set M_1 and the external marker set M_2.

$$M = M_1 \cup M_2 \tag{10}$$

3.2. Watershed segmentation using markers

In the proposed method, the markers have been applied to the gradient image. The gradient image corresponding to the original image is shown in Fig. 1 (b).

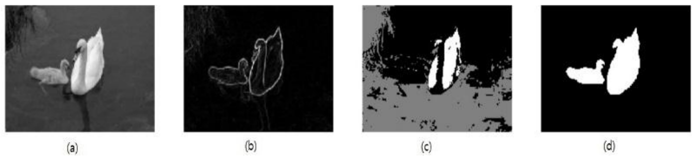

Fig. 1: Procedural steps of the proposed method (a) grayscale image (b) gradient image (c) markers imposed on the gradient image (d) segmentation output of the proposed method

The markers obtained in section 3.1 has been superimposed on the gradient image and Fig. 1 (c) shows the watershed of the gradient image with sources corresponding to the markers. The spatial points marked in gray color ($LB1$) indicate the set of markers (M_1) corresponding to the background, the spatial points marked in white color ($LB2$) indicate the set of markers (M_2) corresponding to the foreground and all the remaining spatial points are represented in black color (0). The coordinates of the modified gradient image can be written as,

$$g_m(x,y) = \begin{cases} LB1, & 0 \le g(x,y) \le k_{R_1} \\ 0, & k_{R_1} < g(x,y) < k_{R_2} \\ LB2, & k_{R_2} \le g(x,y) \le L-1 \end{cases} \tag{11}$$

The spatial points which are labeled in black color are connected to either foreground markers region or background markers region by using the geodesic distance transform in the watershed algorithm. Geodesic distance transform computes the set of all non-labeled pixel points that are at a finite distance from each catchment basin in the gradient image and connects to its closer catchment basin. The following two conditions are useful in attaching the non-labeled pixel point to a catchment basin (CB_m).

1. $d_g\big((x_i,y_i), CB_m\big)$ is finite
2. $d_g\big((x_i,y_i), CB_m\big) < d_g\big((x_i,y_i), CB_n\big)$, for all $m \ne n$

Here, (x_i,y_i) is the spatial position of a non-labeled pixel point and $d_g\big((x_i,y_i), CB_m\big)$ represents the geodesic distance between the pixel's spatial position (x_i, y_i) and the catchment basin CB_m in the gradient image. The condition 1 check whether the pixel point has connectivity to the catchment basin or not and we can find the nearest connected catchment basin for a non-labeled pixel using the condition 2.

The image segmentation process begins when markers are imposed on the gradient image and the final segmentation is obtained when the immersion process on the modified gradient image is completed. The final segmentation of the image using the proposed method is shown in Fig. 1 (d).

4. EXPERIMENTAL ANALYSIS

The proposed method is tested on various images: coins, cameraman, insect, ducks, chain, nature trees, eggs, zebra, breast cancer mammogram, an infrared image of a person and infrared image of a mouse. One mammographic image and two infrared images are considered in order to test the working of the proposed method for the segmentation of mammographic images and infrared images. Fig. 2 shows the original images and their respective histograms. The segmentation results of the proposed method are compared to other segmentation methods: Otsu thresholding method, Edge-based segmentation method, and the traditional watershed segmentation method.

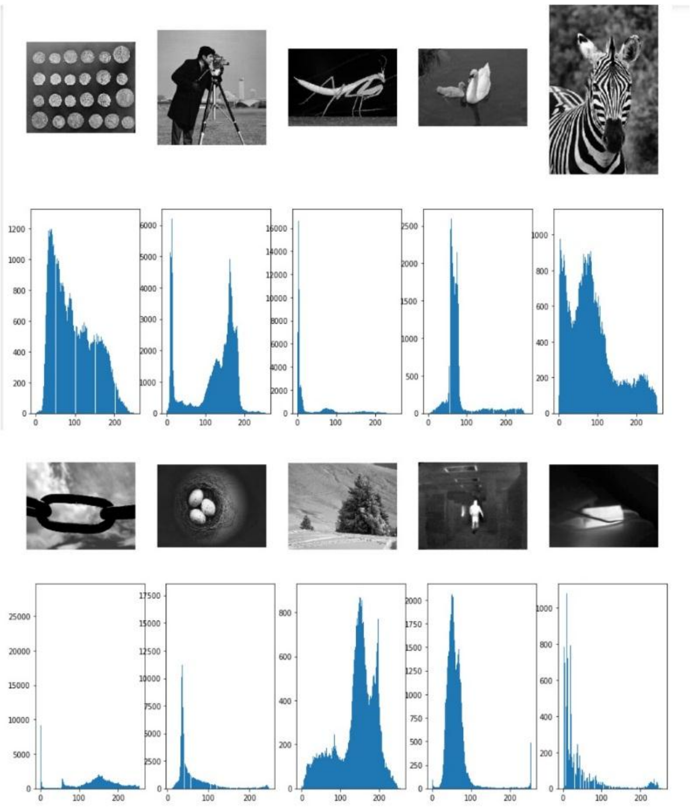

Fig. 2: Original gray images and their corresponding histograms

4.1. Quantitative analysis

In order to analyze the proposed method, the original image has been converted to ground truth image (binary image) by using the thresholding method, for this the threshold value was selected manually. The results have been measured via two quantitative measures: Mean squared error (MSE) [13], and Jaccard index (JI) [16].

Mean squared error

Mean squared error is an image segmentation error. It correlates the segmentation result to the ground truth image. The mathematical expression to find the mean squared error (MSE) between the ground truth image and segmentation result.

$$\mathrm{MSE} = \frac{1}{MN} \sum_{i=1}^{M} \sum_{j=1}^{N} \left(f_T(x,y) - f_O(x,y)\right)^2 \tag{12}$$

Here, the size of the image is $M \times N$, $f_T(x,y)$ represents the intensity of the ground image at a spatial point (x,y) and $f_O(x,y)$ represents the intensity of the segmentation result at a spatial point (x,y). The range of MSE is lies between 0 and 1. The lower value of MSE indicates better segmentation.

Jaccard Index (JI)

JI measures the number of pixels common between the ground truth image and segmentation result by taking the intersection of both and divide it by their union.

$$\mathrm{JI} = \frac{|T \cap O|}{|T \cup O|} \tag{13}$$

Here, O denotes the ground truth image and T denotes the segmentation result. The range of JI lies between 0 and 1. The value of JI is closer to 1 for a good segmentation result and its value is closer to 0 for a bad segmentation result.

4.2. Materials

The proposed method along with the other methods is tested on some images taken from the MSRA database [4], Weizmann database [5]. Infrared images are taken from OTCBVS database [11]. In this paper, the original images without modification are considered for comparing the proposed method with the other image segmentation methods.

4.3. Results and discussions

The segmentation results of the proposed method are compared with the other existing segmentation methods can be seen in Fig. 3. The second column of Fig. 3 shows the segmentation results of the Otsu method. It was observed that segmentation result of the "cameraman" is better compared to the other methods as the histogram exhibits bimodality distribution, while the image "eggs" has a single peak in its histogram (not exhibiting bimodality distribution) that shows some errors in the segmentation result. The third column of Fig. 3 shows the segmentation results of the edge-based segmentation method.

Fig. 3: Image segmentation results of the different methods (a) original gray image (b) Otsu (c) Edge-based (d) Traditional watershed (e) Proposed

This method has given valid segmentation results for the images: coins, ducks and IR2 and it fail to identify the meaningful boundaries between the regions for the remaining images resulting in invalid segmentation results. The fourth column of Fig. 3 shows the segmentation results of the traditional watershed algorithm. The main issue with the traditional watershed algorithm is an over-segmentation problem and it was clearly appeared in these images: coins, cameraman, ducks, nature trees, and IR1. The over-segmentation problem in the traditional watershed algorithm arises due to the presence of invalid regional minima. The proposed method excludes the invalid regional minima and selects only the valid regional minima in terms of the marker set. The last column of Fig. 3 shows the segmentation results of the proposed method. The proposed method has produced some errors for the segmentation of the image "cameraman" and has been succeeded in doing accurate segmentation for the remaining images. This shows the proposed method has the ability to produce accurate segmentation results for multimodal histogram images as well as for the region boundary sensitive images. The proposed method is tested on one mammographic image (MM1) and two infrared images (IR1 and IR2). Our method has successfully identified the tumor in the breast cancer mammographic image (MM1). The image "IR1" shows an infrared image of a man walking in a street and the image "IR2" shows the infrared image of a mouse. We were successful in extracting the objects (man in IR1 and mouse in IR2) in the infrared images. This implies that our method could be used in the segmentation of mammographic images and infrared images.

Table 1: Performance measures of different methods for various types of images

Image	**Method**	**MSE**	**JI**
Coins	Otsu	0.1794	0.5373
	Edge	0.1486	0.5763
	Watershed	0.7986	0.2083
	Proposed	**0.1263**	**0.9138**
Cameraman	Otsu	**0.0217**	**0.9705**
	Edge	0.6632	0.1025
	Watershed	0.2854	0.7145
	Proposed	0.0830	0.8888
Insect	Otsu	0.1112	0.4762
	Edge	0.2684	0.1103
	Watershed	0.3531	0.2226
	Proposed	**0.0311**	**0.7645**
Ducks	Otsu	0.0128	0.8839
	Edge	0.0324	0.7682
	Watershed	0.8915	0.1085
	Proposed	**0.0070**	**0.9368**
Chain	Otsu	0.0979	0.8742
	Edge	0.7333	0.0638
	Watershed	0.1751	0.7989
	Proposed	**0.0426**	**0.9452**
Nature trees	Otsu	0.1137	0.8714
	Edge	0.7549	0.7589
	Watershed	0.8659	0.3840
	Proposed	**0.0931**	**0.8950**
Eggs	Otsu	0.0501	0.5092
	Edge	0.1178	0.1948
	Watershed	0.5454	0.4934
	Proposed	**0.0182**	**0.7551**
Zebra	Otsu	0.0787	0.6783
	Edge	0.2684	0.1103
	Watershed	0.8222	0.1719
	Proposed	**0.0355**	**0.8279**
MM1	Otsu	0.0158	0.5297
	Edge	0.1182	0.0355
	Watershed	0.6845	0.2198
	Proposed	**0.0044**	**0.8021**
IR1	Otsu	0.0043	0.8265
	Edge	0.0468	0.0674
	Watershed	0.1751	0.2989
	Proposed	**0.0012**	**0.9425**
IR2	Otsu	0.0228	0.7447
	Edge	0.0418	0.5530
	Watershed	0.4596	0.1266
	Proposed	**0.0060**	**0.9138**

Table 1 lists the performance measures (MSE and JI) obtained in different methods (Otsu, edge-based, traditional watershed and proposed method) for various images and the best performances have been highlighted to emphasize the significant segmentation method. The proposed method produced valid segmentation results for all images listed in Table 1. It was observed that JI score is more and MSE is less for the Otsu method when compared to the proposed method in case of "cameraman" image. These results showed that the Otsu method is the most suitable method for the segmentation of the images having bimodal distribution histograms. However, the proposed method was performed well for the other remaining images. We have obtained MSE value very close to 0 for the images: ducks, MM1, IR1 and IR2, and JI score close to 1 for the images: coins, ducks, chain, IR1, and IR2 in the proposed method. These results show the significance of the proposed method in the image segmentation applications.

We implemented the proposed method on a PC with Intel Corei7, 3.6 GHz processor and 8 GB RAM. The experiments were conducted in Python programming environment. The average running time of our proposed method for image segmentation is 0.639 s and it is an optimistic computation time for the image segmentation in image processing.

5. CONCLUSION

In this paper, we propose a new, robust, accurate and automatic marker generation algorithm to implement a completely automatic markers-based watershed algorithm. The algorithm needs no prior information for selecting internal and external markers. By using the details of gray-scale image histogram and Otsu threshold information we find the markers and we apply the markers to the morphological watershed algorithm for getting image segmentation. We have obtained accurate quantitative results demonstrating the robustness of our marker generation method.

ACKNOWLEDGMENT

This research was financially supported by the Ministry of Trade, Industry and Energy (MOTIE) and Korea Institute for Advancement of Technology (KIAT) through the National Innovation Cluster R&D program (P0006704_Development of energy saving advanced parts).

REFERENCES:

[1] W. Jianlai, Y. Chunling, Z. Min, W. Changhui, Implementation of otsu's thresholding process based on FPGA, 2009 4th IEEE Conf. Ind. Electron. Appl. ICIEA 2009. 1 (2009) 479–483. doi:10.1109/ICIEA.2009.5138252.

[2] T. Porter, E.R. Dougherty, Mathematical Morphology in Image Processing, Math. Gaz. 78 (2007) 229. doi:10.2307/3618604.

[3] N. Nausheen, A. Seal, P. Khanna, S. Halder, A FPGA based implementation of Sobel edge detection, Microprocess. Microsyst. 56 (2018) 84–91. doi:10.1016/j.micpro.2017.10.011.

[4] P. Parida, N. Bhoi, Transition region based single and multiple object segmentation of gray scale images, Eng. Sci. Technol. an Int. J. 19 (2016) 1206–1215. doi:10.1016/j.jestch.2015.12.009.

[5] S. Alpert, M. Galun, A. Brandt, R. Basri, Image segmentation by probabilistic bottom-up aggregation and cue integration, IEEE Trans. Pattern Anal. Mach. Intell. 34 (2012) 315–327. doi:10.1109/TPAMI. 2011.130.

[6] H.G. Kaganami, Z. Beiji, Region-based segmentation versus edge detection, IIH-MSP 2009 - 2009 5th Int. Conf. Intell. Inf. Hiding Multimed. Signal Process. (2009) 1217–1221. doi:10.1109/IIH-MSP.2009.13.

[7] J. Chen, B. Guan, H. Wang, X. Zhang, Y. Tang, W. Hu, Image Thresholding Segmentation Based on Two Dimensional Histogram Using Gray Level and Local Entropy Information, IEEE Access. 6 (2017) 5269–5275. doi:10.1109/ACCESS.2017.2757528.

[8] R.E. Gonzalez, Rafael and Woods, Digital_Image_Processing_2ndEdb.pdf, (n.d.).

[9] N. Otsu, P. Smith, D.B. Reid, C. Environment, L. Palo, P. Alto, P.L. Smith, Otsu_1979_otsu_method, C (1979) 62–66. doi:10.1109/TSMC.1979.4310076.

[10] X. Ji, Y. Li, J. Cheng, Y. Yu, M. Wang, Cell image segmentation based on an improved watershed algorithm, Proc. - 2015 8th Int. Congr. Image Signal Process. CISP 2015. 1 (2016) 433–437. doi:10.1109/CISP.2015.7407919.

[11] T. Wu, R. Hou, Y. Chen, Cloud Model-Based Method for Infrared Image Thresholding, Math. Probl. Eng. 2016 (2016) 1–18. doi:10.1155/2016/1571795.

[12] M. Malarvel, G. Sethumadhavan, P.C.R. Bhagi, S. Kar, S. Thangavel, An improved version of Otsu's method for segmentation of weld defects on X-radiography images, Optik (Stuttg). 142 (2017) 109–118. doi:10.1016/j.ijleo.2017.05.066.

[13] S.M. Elbayoumi Harb, N.A.M. Isa, S.A. Salamah, Improved image magnification algorithm based on Otsu thresholding, Comput. Electr. Eng. 46 (2015) 338–355. doi:10.1016/j.compeleceng.2015.03.025.

[14] S. Umaa Mageswari, M. Sridevi, C. Mala, An experimental study and analysis of different image segmentation techniques, Procedia Eng. 64 (2013) 36–45. doi:10.1016/j.proeng.2013.09.074.

[15] H. Fan, F. Xie, Y. Li, Z. Jiang, J. Liu, Automatic segmentation of dermoscopy images using saliency

combined with Otsu threshold, Comput. Biol. Med. 85 (2017) 75–85. doi:10.1016/j.compbiomed.2017.03.025.

[16] P. Parida, N. Bhoi, Wavelet based transition region extraction for image segmentation, Futur. Comput. Informatics J. 2 (2017) 65–78. doi:10.1016/j.fcij. 2017.10.005.

[17] M. Veta, A. Huisman, M.A. Viergever, P.J. Van Diest, J.P.W. Pluim, Marker-controlled watershed segmentation of nuclei in H&E stained breast cancer biopsy images, Proc. - Int. Symp. Biomed. Imaging. (2011) 618–621. doi:10.1109/ISBI.2011.5872483.

[18] L. Gao, S. Yang, J. Xia, J. Liang, Y. Qin, A new marker-based watershed algorithm, IEEE Reg. 10 Annu. Int. Conf. Proceedings/TENCON. 2 (2007) II–81. doi:10.1109/TENCON.2006.343747.

[19] G.N. Girish, A. R. Kothari, J. Rajan, Marker controlled watershed transform for intra-retinal cysts segmentation from optical coherence tomography B-scans, Pattern Recognit. Lett. 0 (2018) 1–9. doi:10.1016/j.patrec. 2017.12.019.

[20] S. Lu, S. Wang, Y. Zhang, A note on the marker-based watershed method for X-ray image segmentation, Comput. Methods Programs Biomed. 141 (2017) 1–2. doi:10.1016/j.cmpb.2017.01.014.

[21] D. Li, G. Zhang, Z. Wu, L. Yi, An edge embedded marker-based watershed algorithm for high spatial resolution remote sensing image segmentation, IEEE Trans. Image Process. 19 (2010) 2781–2787. doi:10.1109/TIP.2010.2049528.

[22] M.H. Malik, T. Zhang, H. Li, M. Zhang, S. Shabbir, A. Saeed, Mature Tomato Fruit Detection Algorithm Based on improved HSV and Watershed Algorithm, IFAC-PapersOnLine. 51 (2018) 431–436. doi:10.1016/j.ifacol. 2018.08.183.